

Pierre Durand¹, Jean-Luc Attié², Dominique Lambert² Grégoire Pigeon¹¹CNRM (Météo-France-CNRS), Toulouse, France ; ²Lab. d'Aérodologie (UPS-CNRS), Toulouse, France

1. INTRODUCTION

During the one-year CAPITOUL urban experiment (see Masson et al., 2004), performed in and around the urban area of Toulouse (France) between Feb. 2004 and Feb. 2005, continuous measurements of the surface energy budget are performed at a rural and a down-town site. Moreover, CO₂ flux was measured at the urban site. The sensible heat, latent heat and CO₂ fluxes were computed with the eddy-correlation technique. In addition, raw time-series were analysed with a wavelet transform, using the conditional analysis developed by Galmarini and Attié (2000) and Attié and Durand (2003). Some illustrations are given in this paper, in order to highlight differences between urban and rural transfer processes, and to illustrate the behaviour of the urban CO₂ flux.

2. MEASUREMENTS

In the old city center of Toulouse, a telescopic mast was installed on the terrace-roof of a 20m high building. The head of the mast stand at either 18 or 28m above the terrace, according to wind conditions. It is equipped with a sonic Gill anemometer measuring the 3D wind and the so-called sonic temperature, and a LiCor 7500 measuring the fluctuations of H₂O and CO₂ concentration. At the rural site (a flat agricultural parcel located 40km NW of the city), a 10m mast is equipped with a 3D sonic anemometer, and a Campbell KH20 fast hygrometer. On both sites, the data are sampled at a rate of 20s⁻¹.

3. DATA PROCESSING

Fluxes were calculated with the conventional eddy-correlation technique on 30min samples, from the 20s⁻¹ detrended time-series (Pigeon et al., 2004). We also used in this paper 24h time-series, reduced by averaging at a rate of 0.25s⁻¹. Although the undersampling of the time-series probably results in a slight underestimation of the flux, this allows us to analyse the variation of the transfers through the whole diurnal cycle. These time-series were high-pass filtered, with a recursive filter (McMillen, 1988) using a time constant of 900s (i.e., a cut-off period of about 90min.). This operation removes from the signals the large fluctuations related to the diurnal variation, and allows us to focus on the transfer processes.

The conditional wavelet technique (CWT) combines the wavelet transform with conditional sampling, as described by Attié and Durand (2003). We apply this technique for analysing the fluxes.

The wavelet cross-scalogram shows a cross-spectral representation of the transfer in a time-frequency diagram. Then, the sign of each variable wavelet transform (for example, vertical velocity and temperature for the heat flux) is indicated by four colors (classes). So, the main wavelengths (or frequencies) contributing to the transfers and each kind of parcels (warm updrafts, dry downdrafts, etc.) are detecting.

4. URBAN FLUX ON SELECTED DAYS

The transfers of heat, water vapour and CO₂ on the city are illustrated on three cloud-free selected days, one at the end on the winter (March, 10, with temperature between 1 and 8°C), the two others in spring (21st and 25th of April, with temperature between 9 and 22°C, and between 10 and 21°C, respectively). The heat release from anthropogenic source is therefore higher on the first day. The 25th April is a Sunday, with low traffic, whereas the two other days are in the middle of the week. The flux values, as well as the wind speed, averaged over the day, are presented in the Table below.

	Mar. 10	Apr. 21	Apr. 25
Wind (m/s)	2.7	4.6	1.2
Sensible heat flux (W/m ²)	82	68	83
Latent heat flux (W/m ²)	21	15	18
CO ₂ flux (mg m ⁻² s ⁻¹)	1.56	0.69	0.34

The analysis of the transfers are illustrated on Figs. 1 (March, 10, hereafter D1), 2 (April, 21, hereafter D2) and 3 (April, 25, hereafter D3). The time-series of the vertical velocity reveals comparable turbulence intensities during the daytime on the three days (upper diagrams). However, the daytime turbulence on D1 and D3 is from thermal origin (buoyancy), and the instantaneous covariance w'T' presents high positive values (warm updrafts). On D2, the wind is stronger, and this mechanical source of turbulence ensures positive and negative fluctuations of w'T'. However, the sensible heat flux has comparable values on the three days. Starting from the top of each figure, the 2nd, 4th and 6th plots represent the instantaneous covariance (w'T', w'q' and w'CO₂', respectively) as well as the

* Corresponding author address: Pierre Durand, CNRM, 42 av. G. Coriolis, 31057 Toulouse Cedex 1. Pierre.Durand@meteo.fr

corresponding time integrals, whose the variation of the slope translates the corresponding flux variation. One can see that the heat flux presents high values during daytime, and remains slightly positive during nighttime (in the range $0-20\text{W/m}^2$), due to the release of heat stored in the housings during the day, and to the anthropogenic heat source (mainly on D1). Not surprisingly, latent heat flux is weak, peaking at about 60W/m^2 on D2 and D3. Conversely, CO_2 flux values are high, mainly on D1 (wintertime middle week day). They are five times lower on D3, which is a Sunday without domestic heating and with low traffic, whereas D2 is the intermediate case (high traffic and no domestic heating). One can note that the flux remains positive at night, with same order values on D1 and D3 as those averaged on the whole day. However, D1 exhibits several spikes during morning, which correspond to the period of the highest flux (between 7h and 10h UTC). High values are also observed in the morning of D2, but not on D3, due to the traffic reduction. If we look at the raw CO_2 time-series (not shown here), we observe that the highest values are reached at the end of the night. There is a quite sudden decrease in the morning when turbulence starts to mix CO_2 in the boundary layer; and then a continuous increase up to the end of the following night. This increase is weak during the morning (for the middle week day) and up to the middle of the afternoon during Sunday (D3), when turbulence is strong enough and/or sources weak enough to prevent accumulation.

Conditional wavelets (3^{rd} , 5^{th} and 7^{th} diagrams on the figures) illustrates the differences between the various transfers: the main information concentrates on the middle of the day for the sensible heat flux, whereas it is located in the morning for the CO_2 flux. The blue and red colors translate as upward transfer (either positive or negative fluctuations in both w and the corresponding scalar), whereas green and yellow translate as negative. Note that, during daytime, upward areas can be observed on the three fluxes (at frequencies of around 0.01Hz), whereas, at lower frequencies, upward latent heat flux and downward sensible heat flux can be observed. This is a signature of large eddies entrained from the top of the boundary-layer (where positive temperature and negative moisture jumps are present) down to the surface-layer. At the same frequencies, the CO_2 flux wavelet diagram does not present any systematic behaviour, which probably translates as the absence of a systematic jump in CO_2 at the top of the urban boundary layer.

5. URBAN VS. RURAL FLUX

Figure 4 illustrates one of the most striking difference between urban and rural flux: it presents the nighttime heat flux, over a 1-hour sample (from 0h to 1h UTC), measured on D2 at the two sites. The time-integral of the covariance reveals a negative flux at the rural site, as expected (it reaches -5W/m^2), whereas it is the opposite at the urban one. In the latter case, the heat is transported by both a continuous turbulence, and some isolated spikes coming from local heat releases

(anthropogenic sources). The conditional wavelet diagram reveals the areas of the positive contribution (blue and red), located along the whole sample, but on the ten first and ten last minutes. At the rural site, the nocturnal cooling develops a stable stratification (inversion layer close to the ground). The 1-hr sample clearly exhibits two different parts: during the first half-time, there is no significant flux; the conditional cross-scalogram shows a regular alternance of the four classes (yellow, green, red, blue, yellow, etc.) probably due to gravity waves whose frequency is about 0.002Hz . On the second half-time, the turbulence increases and the flux becomes significant, with a majority of green and yellow areas on the conditional cross-scalogram.

6. REFERENCES

- Attié, J.L. and Durand, P., 2003, *Conditional wavelet method applied to aircraft data measured in the thermal internal boundary layer during sea-breeze events*. **Bound. Layer Meteorol.**, **106**, 359-382.
- Galmarini, S. and Attié, J.L., 2000, *Turbulent transport at the thermal internal boundary layer top: Wavelet analysis of aircraft measurements*. **Bound. Layer Meteorol.**, **94**, 175-196.
- Masson, V., G. Pigeon, P. Durand, L. Gomes, J.A. Salmond, J.P. Lagouarde, J.A. Voogt, T.R. Oke and C. Lac, 2004, *The Canopy and Aerosol Particles Interactions in Toulouse Urban Layer (CAPITOUL) experiment: first results*. **Fifth Conference on Urban Environment**, Vancouver BC, Ca., 23-27 Aug.
- McMillen, 1988, *An eddy-correlation technique with extended applicability to non-simple terrain*. **Bound.-Layer meteorol.**, **43**, 231-245.
- Pigeon, G., C. Augustin, D. Legain, V. Masson and P. Durand, 2004, *Characteristics of the urban thermodynamic island and the energy balance on Toulouse (France) during winter and spring periods of the CAPITOUL experiment*. **Fifth Conference on Urban Environment**, Vancouver BC, Ca., 23-27 Aug.

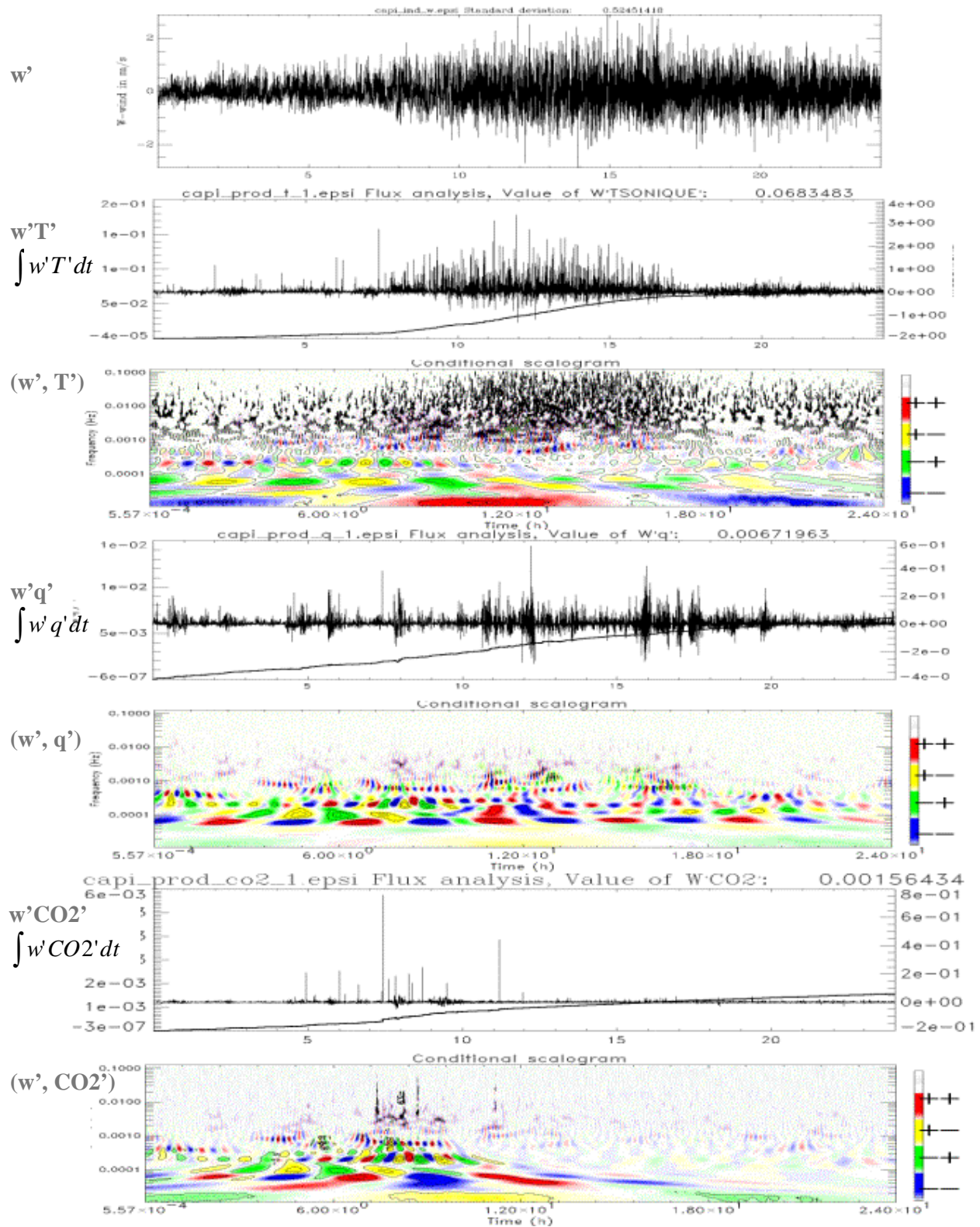


Figure 1: Time series and flux wavelet conditional scalograms for March, 10. From top to bottom: vertical velocity w , instantaneous covariance $w'T'$ and its time-integral, cross-scalogram of (w', T') , instantaneous covariance $w'q'$ and its time-integral, cross-scalogram of (w', q') , instantaneous covariance $w'CO_2'$ and its time-integral, cross-scalogram of (w', CO_2')

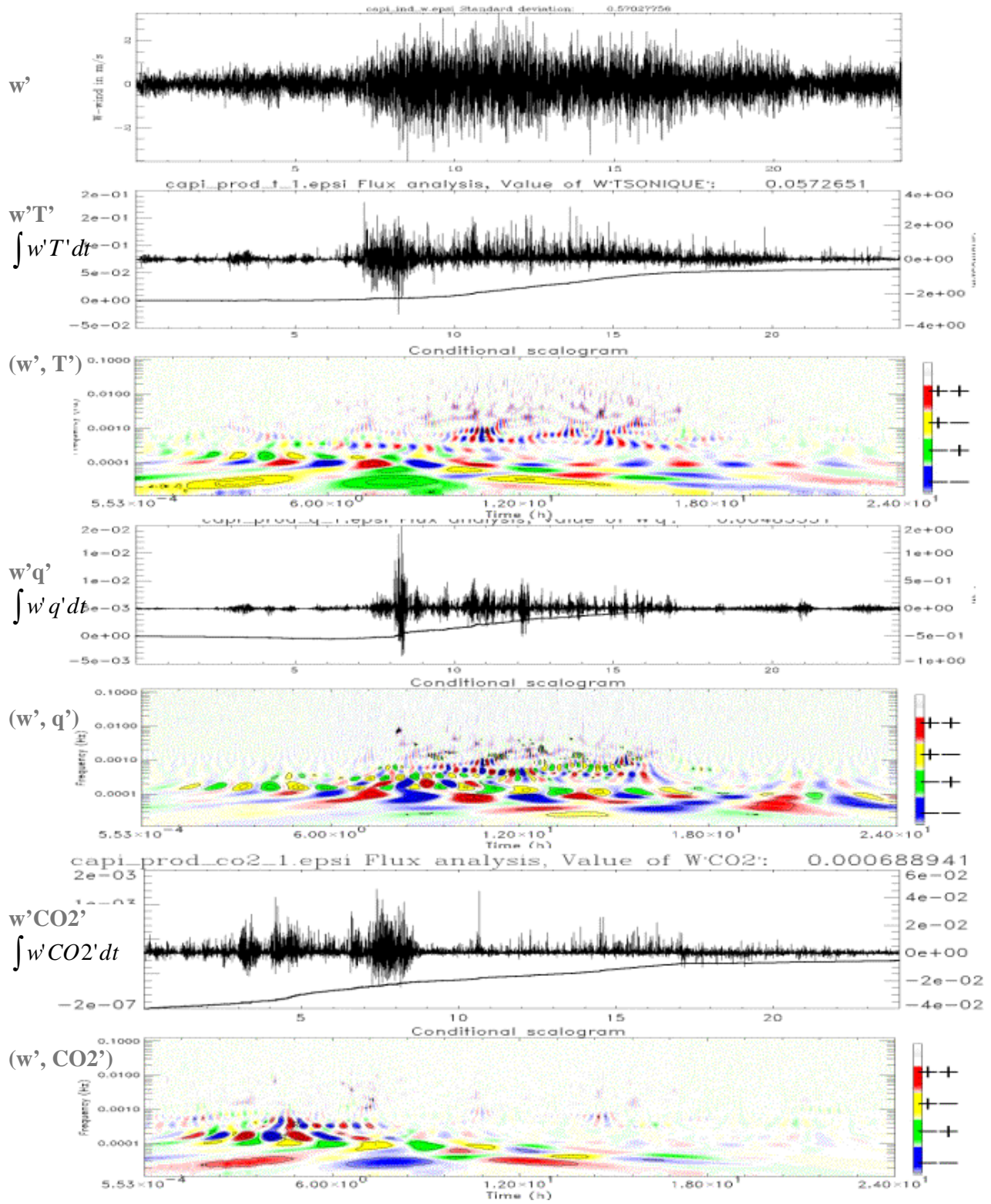


Figure 2: Same as Fig. 1, but for April, 21.

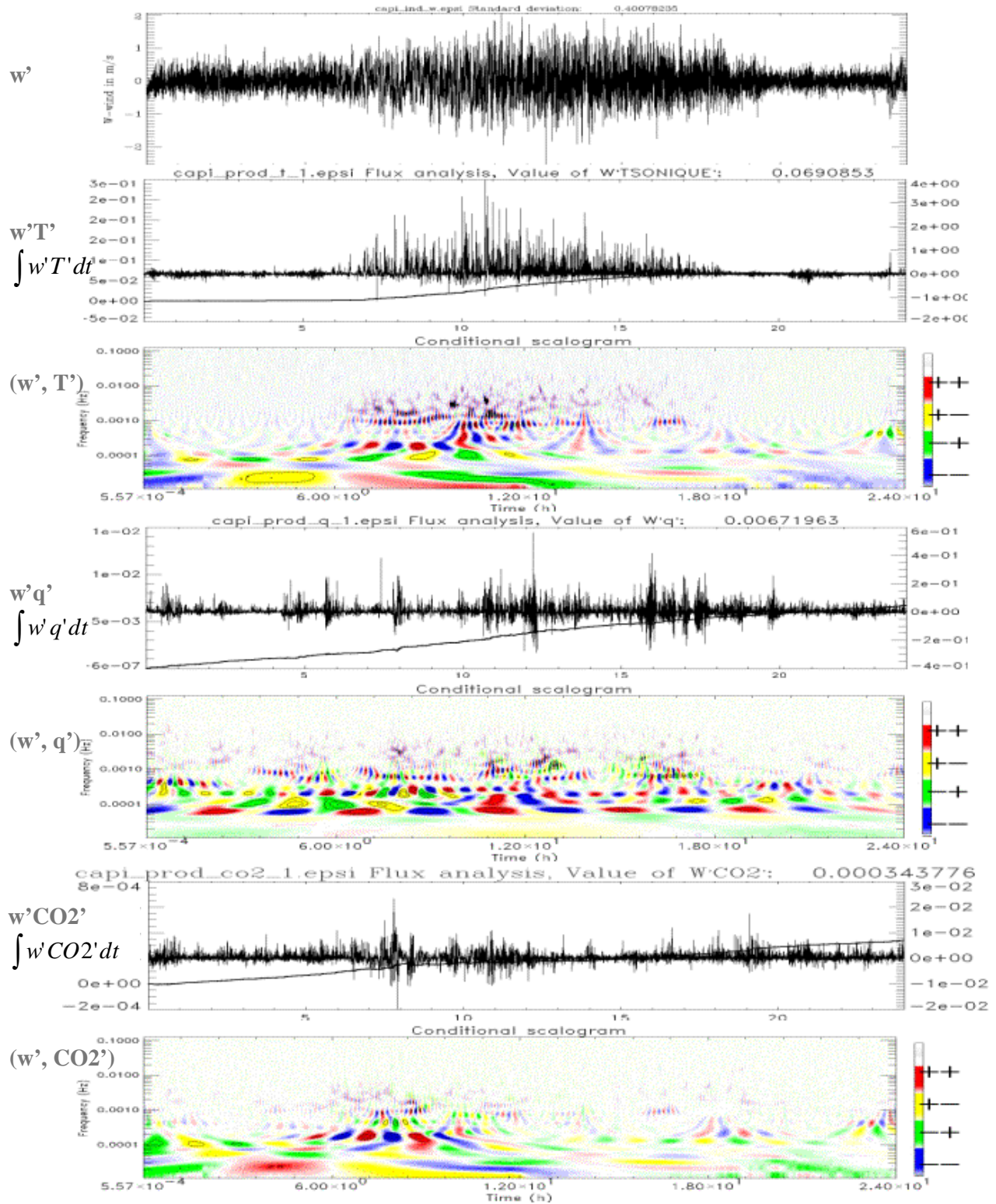
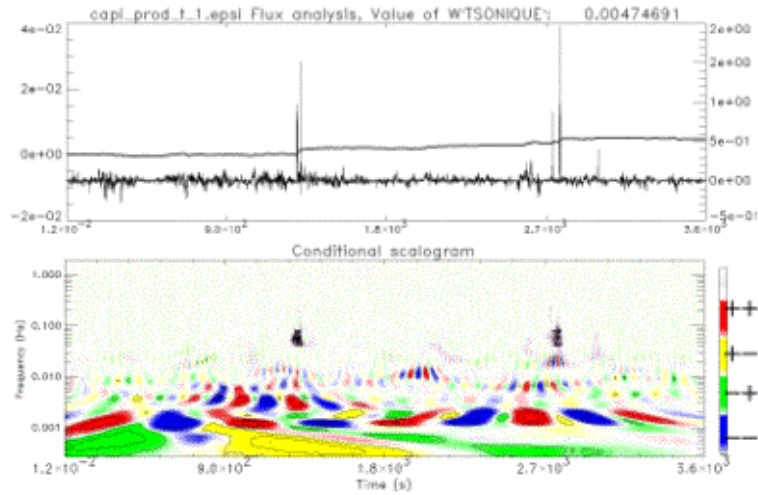


Figure 3: Same as Fig. 1, but for April, 25.

$$w'T'$$

$$\int w'T' dt$$

Urban site

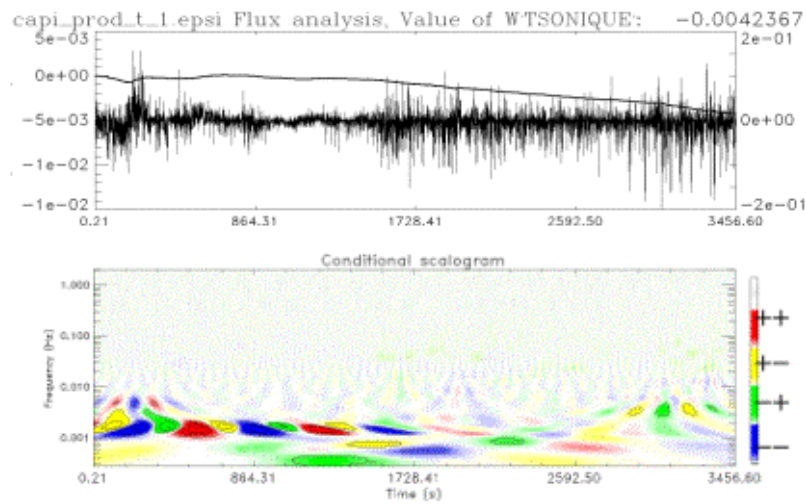


(w', T')

$$w'T'$$

$$\int w'T' dt$$

Rural site



(w', T')

Figure 4: Time series and wavelet conditional scalograms for heat flux at the urban (two upper diagrams) and rural (two lower diagrams) sites. April, 21, between 0h and 1h UTC.